Complex Optical Constants on a Subwavelength Scale

R. Hillenbrand and F. Keilmann*
Max-Planck-Institut für Biochemie, 82152 Martinsried, Germany
(Received 7 April 2000)

Optical phase contrast has for the first time been observed on a nanometer scale, with a near-field microscope of scattering type that maps the complete optical field of amplitude *and* phase. Backed by quasielectrostatic theory, we demonstrate the significance and experimental accessibility of even complex optical constants on a subwavelength scale. Further, our method can separate the near-field response from background artifacts and thus is expected to enable nanoscale optical mapping of even topography-rich objects such as resonant clusters and macromolecules.

PACS numbers: 77.22.–d, 07.79.Fc, 78.20 Ci

Optical constants are definable down to a scale where a material's charge or dipole densities cease to be continuous, usually much below an optical wavelength, and can in principle be studied towards this limit by scanning near-field optical microscopy (SNOM) that allows optical probing on a subwavelength scale. A resolution of 1 nm has been attained in the scattering-type version (s-SNOM) which records light scattered from the apex of a sharp "apertureless" probing tip [1]. In this microscope the phase of the near field has not yet been exploited (with the exception of microwave-operated s-SNOMs [2–5]). This is surprising because phase contrast is in classical microscopy of well-established, unique value for many fields of science. Distinct phase effects can be expected for resonant interactions such as absorption, lasing, or resonant scattering. The significance of the near-field phase is illustrated by light-scattering calculations predicting "phase confinement" [6], i.e., strong phase variations on a subwavelength scale near small objects [7]. Here we show that simultaneous amplitude and phase nanoscale imaging is possible in s-SNOM, by using an interferometer to completely characterize the scattered light, much in the fashion of other dual-channel optical techniques such as ellipsometry. We observe a definite near-field material contrast between Au and Si, both in amplitude and phase, as it is predicted from quasielectrostatic theory using macroscopic optical constants. The measurement crucially rests on a new procedure to detect the near-field response even in the presence of strong background scattering.

Our microscope (Fig. 1) uses a stabilized 633 nm HeNe laser of which about 0.1 mW reaches a commercial cantilevered Si tip (Silicon-MDT, Moscow), Au coated with radius of curvature $\approx$20 nm through an aspheric lens with 0.25 numerical aperture, at an incidence angle 60° off the tip axis. The electric field $E_i = E_0 e^{-i\omega t}$ is polarized in the incidence plane. Backward-scattered light is collected with the same lens and directed to a fast detector (1801, New Focus, Santa Clara). The tip is fixed but dithers vertically with amplitude $\Delta z \approx 20$ nm at the cantilever resonance $\Omega \approx 45$ kHz [tapping mode AFM (atomic force microscope)]. The sample is xyz scanned by a calibrated piezoelectric stage (Physik Instrumente, Waldbronn). Unambiguous phase detection of the scattered wave $E_{\mathrm{sca}} \propto E_i$ is performed by a heterodyne scheme that superimposes a coherent wave $E_{\mathrm{ref}} \propto e^{-i\Delta t} E_i$ with frequency shifted by Δ (in our experiment $\Delta =$ 80 MHz). The 80 MHz component of the detector signal $U \propto |E_{\mathrm{sca}}|^2 + |E_{\mathrm{ref}}|^2 + 2|E_{\mathrm{sca}} E_{\mathrm{ref}}| \cos(\Delta t + \varphi)$ is filtered by a dual-output lock-in amplifier (SRS 844, Stanford Research Systems, Sunnyvale) which determines amplitude and phase simultaneously. Note that this phase equals the optical phase φ and that the amplitude $2|E_{\mathrm{sca}} E_{\mathrm{ref}}|$ exceeds $|E_{\mathrm{sca}}|^2$ (the amplitude expected for direct detection) by the heterodyne amplification factor $2|E_{\mathrm{ref}}/E_{\mathrm{sca}}|$, here about 3 orders of magnitude.

For calculating the optical near-field response of the s-SNOM, including the phase, we model the tip by a point dipole [1,8,9] with polarizability $\alpha = 4\pi a^3 (\varepsilon_t - 1)/(\varepsilon_t + 2)$, where $a \ll \lambda$ and ε_t are the tip's radius of curvature and complex dielectric constant, respectively. With the tip's apex at distance $z \ll \lambda$ above a half-space sample material characterized by its macroscopic dielectric constant ε_s, the sample's polarization is represented by an image dipole with polarizability $\alpha\beta = \alpha(\varepsilon_s - 1)/(\varepsilon_s + 1)$, and the combined polarizability of both becomes [8,10]

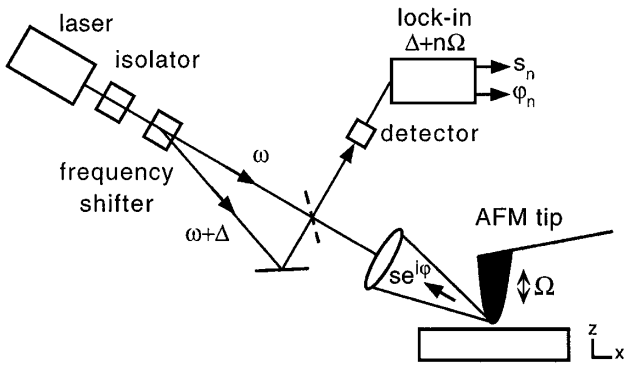

FIG. 1. Sketch of complex-contrast s-SNOM (*scattering* scanning near-field optical microscope) containing an optical interferometer with an acousto-optic frequency shifter, a reflection path which couples to an AFM tip z dithered at Ω, and a vector lock-in amplifier operating at the sum frequency of either $\Delta + \Omega$ or $\Delta + 2\Omega$.

$$\alpha_{\text{eff}} = \frac{\alpha(1+\beta)}{1 - \frac{\alpha\beta}{16\pi(a+z)^3}}. \quad (1)$$

Hence the scattered far field $E_{\text{sca}} = \alpha_{\text{eff}}\pi\sqrt{8\pi/3}/\lambda^2 E_i = \sigma E_i$ directly measures both the amplitude s and the phase φ of the complex near-field interaction $\sigma = s\,e^{i\varphi}$ (note SNOMs measure a material-dependent interaction since the probe is a scattering source that influences the object's illumination and near fields). The result for an Au tip (Fig. 2) shows that enhanced amplitudes are accompanied by a marked phase increase as the wavelength tunes through the small-Au-particle plasmon resonance near 540 nm. The s-SNOM contrast in this case varies strongly over the spectrum, and it happens that near 500 nm the phase distinguishes an Au sample from an Ag sample, whereas the amplitude does not.

In a real s-SNOM the shaft of the tip (and also the end of the cantilever, if illuminated) presents a second, background source σ^b of light scattering which adds coherently to σ. Suppression of σ^b is a crucial task since σ^b is typically strong and varies with z on scale λ because of interference fringes parallel to the surface, owing to the fact that illuminating (or collecting from) the scattering source occurs either directly or via a surface reflection. If σ^b remains large, any tip motion in z, such as it occurs in the topography-following AFM mode, induces a "z-motion" artifact in the optical image. Fortunately, since σ varies in a nonlinear fashion [Eq. (1)] in the narrow near-field range $0 < z \le a \ll \lambda$, z dithering of the tip and signal demodulation at frequency Ω [11] can be used to enhance the near field over the background contribution. In our experiment below, however, this does not yet suffice to suppress the background completely (Fig. 3). Further suppression is achievable by choosing the harmonic 2Ω for lock-in demodulation [12]. In general, it is the nonlinearity in $\sigma(z)$ that generates harmonics described by the Fourier series of σ (and likewise σ^b),

$$\sigma = \sigma_0 + \sigma_1\cos(\Omega t) + \sigma_2\cos(2\Omega t) + \ldots, \quad (2)$$

where σ_n is proportional to the nth z derivative of σ in the case of small dither amplitude $\Delta z \ll a$. The different scales of z dependence enhance the near-field over the background terms with rising n, as shown by numerical simulation and experiments [10]. Note that the common direct detection scheme [8,10,13,14] detects $U \propto |\sigma + \sigma^b|^2$ and thus measured mainly products between near field and background, even at large n [10,15]. Our heterodyne scheme, in contrast, avoids such obviously distorting products since it extracts the $\Delta + n\Omega$ modulated component out of the detector signal $U \propto |\sigma + \sigma^b + e^{i\Delta t}|^2$, yielding the single complex sum $\sigma_n + \sigma_n^b = s_n e^{i\varphi_n} + s_n^b e^{i\varphi_n^b}$. In our experiment the second term vanishes already at $n = 2$ so that the pure near-field amplitude and phase result.

A pure near-field response is demonstrated in Fig. 4(b), which maps repeated z scans while a well-defined test sample slowly moves in x. Here demodulation at $\Delta + 2\Omega$ has reduced the background completely, while the image taken with demodulation at $\Delta + \Omega$ [Fig. 4(a)] shows considerable background, similar to Fig. 3. This is in excellent agreement with the analysis above. The near-field amplitude is clearly enhanced at the Au surface compared to Si. The scale of the near-field interaction in z is about 20 nm, of the same order as a (tip radius); it is expected to decrease with n and thereby improve the lateral resolution

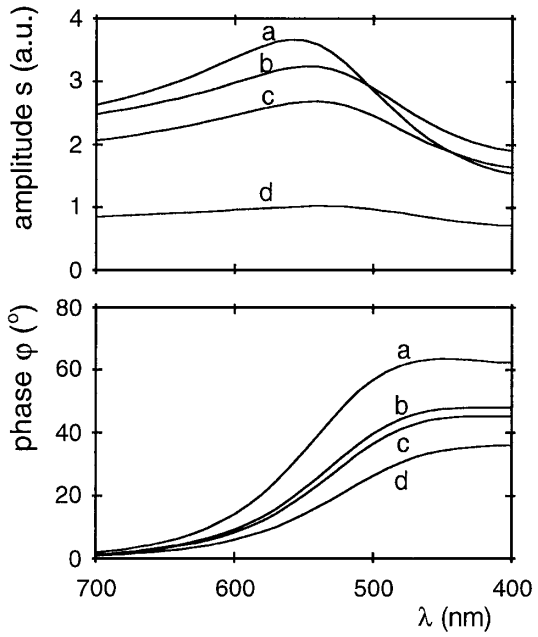

FIG. 2. Calculated optical amplitude and phase response vs wavelength, of a small ($a \ll \lambda$) Au sphere contacting an (a) Au, (b) Ag, and (c) Si surface; (d) no sample (Mie scattering).

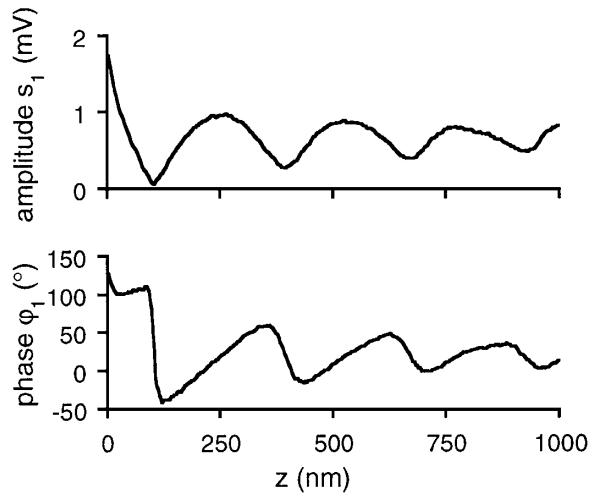

FIG. 3. Measured optical amplitude and phase response vs distance z between tip and Au sample (approach curves, demodulation at $\Delta + \Omega$), showing narrow extent of near field ($z \le 40$ nm) in both observables, and long-range standing-wave background.

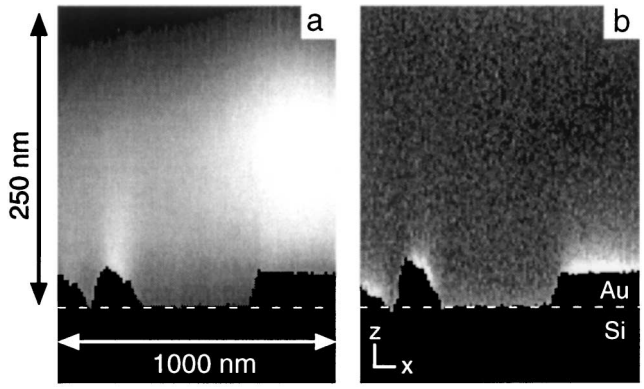

FIG. 4. Optical amplitude response (x-z scans) of a metal AFM tip over a well-defined test sample, a nanostructured, 25 nm high Au layer evaporated on Si (300 nm polystyrene spheres were used as a temporary evaporation mask). The AFM topography is depicted as black basis. Demodulation (a) at $\Delta + \Omega$ yields a signal dominated by background scattering, while demodulation (b) at $\Delta + 2\Omega$ singles out the near-field contribution.

[10]. About 20 nm edge resolution is demonstrated in σ_2 images of the same sample (Fig. 5), obtained by setting the feedback to stabilize at 90% of the free dither amplitude (constant-distance mode).

For a quantitative determination of material contrast we plot the experimental vector sums $\sigma_n + \sigma_n^b$ vs z (approach curves) on a polar diagram (Fig. 6) where the polar angle represents the optical phase. The signal $\sigma_1 + \sigma_1^b$ [Fig. 6(a)] describes distorted circular trajectories, evidence of dominating background (both the form and location of these trajectories vary with fine adjustment of the lens, not shown). Extrapolation of trajectories is tried by fitting spirals to the range $2a < z < \lambda$, the difference from which in the range $z < 2a$ is interpreted as the near-field contribution σ_1 and plotted in Fig. 6(b). As a result, we find that the near field has a distinct phase which varies relatively weakly with z, and this phase is distinctly different for the two materials. Besides, we note that the phase difference between near field and background is rather arbitrary and changes with fine adjustment of the lens.

In a subsequent experiment the optical signal $\sigma_2 + \sigma_2^b$ is independently measured and displayed in Fig. 6(c) without any background subtraction. Only very small circular trajectories, not visible in Fig. 6(c), are found in this signal,

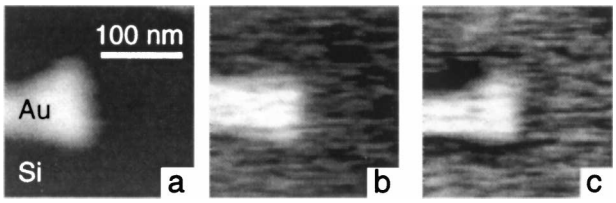

FIG. 5. Simultaneously recorded x-y images of sample as in Fig. 4, showing (a) AFM topography, (b) optical amplitude, and (c) optical phase; demodulation at $\Delta + 2\Omega$.

confirming an effective background suppression and therefore a much improved near-field determination, owing to the $\Delta + 2\Omega$ demodulation. The near-field response σ is obtained only within an arbitrary phase factor, i.e., with arbitrary rotation around the origin, due to an undetermined path length difference d of the heterodyne interferometer, $d \approx 10$ cm $\gg \lambda$. Because of the Invar base plate in our setup the temperature drift of d remains below $\lambda/300$ over several sec, sufficient to allow a meaningful phase comparison within an image and between successive images.

Relative near-field material contrasts $\sigma_n(\mathrm{Au})/\sigma_n(\mathrm{Si})$ resulting from the data in Figs. 6(b) and 6(c) are plotted

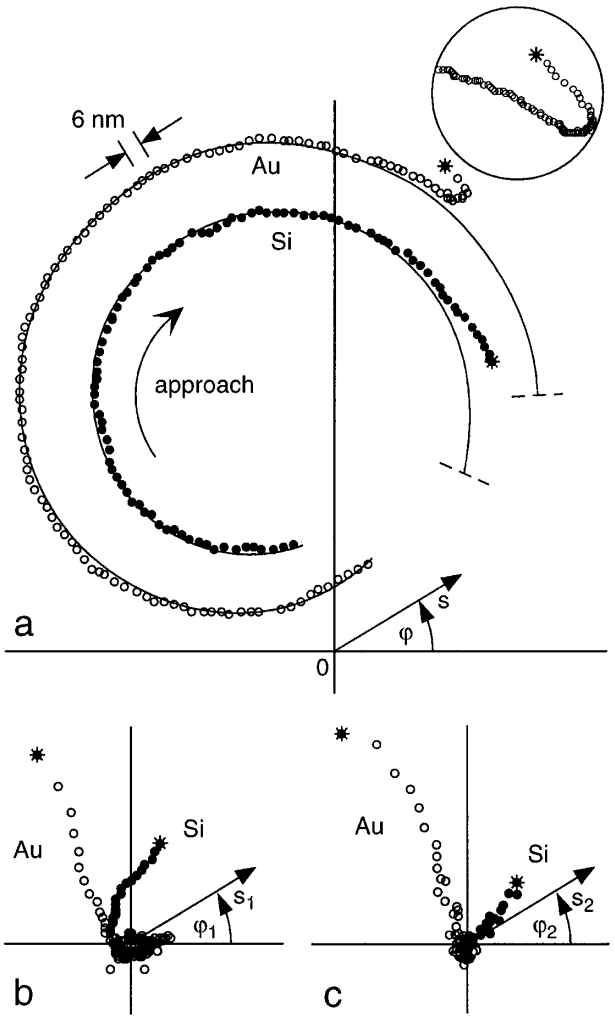

FIG. 6. Polar display of measured optical amplitude and phase response vs approach of Si (full dots) or Au (open dots) sample; contact is depicted as an asterisk (*); data are taken every 0.6 nm but only every fifth is shown, thus giving the z scale: (a) response demodulated at $\Delta + \Omega$, with enlarged view of trajectory near contact showing each data point, and with extrapolation to contact (dashed line) of spiral trajectory (full curve) interpreted as background component; (b) near-field response obtained from measured data (a) by subtracting extrapolation; (c) near-field response demodulated at $\Delta + 2\Omega$ (unprocessed, data taken every 0.2 nm, every tenth shown).

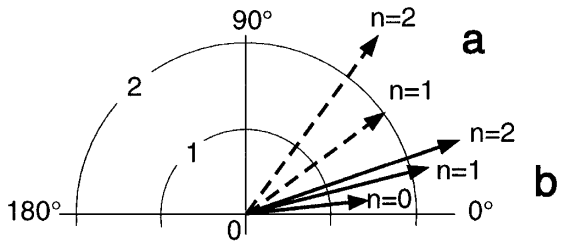

FIG. 7. Complex optical near-field contrast between Au and Si sample material, $\sigma_n(\mathrm{Au})/\sigma_n(\mathrm{Si})$: (a) taken from experiment, Figs. 6(a) and 6(c) (dashed vectors); (b) calculated with Eq. (1) for 633 nm wavelength, using $\varepsilon_{\mathrm{Au}} = -10 + 4i$, $\varepsilon_{\mathrm{Si}} = 15$ (full vectors).

in Fig. 7 (the unit vector $1e^{i0}$ means no contrast). They amount to $s_2(\mathrm{Au})/s_2(\mathrm{Si}) = 2.5 \pm 0.1$ and $\varphi_2(\mathrm{Au}) - \varphi_2(\mathrm{Si}) = 60° \pm 10°$. For σ_1 the results are somewhat less certain due to the extrapolation, $s_1(\mathrm{Au})/s_1(\mathrm{Si}) = 2 \pm 0.2$ and $\varphi_1(\mathrm{Au}) - \varphi_1(\mathrm{Si}) = 40° \pm 20°$. We compare these measured near-field optical contrasts with those predicted from our model by differentiating Eq. (1). As seen in Fig. 7 both the measured and calculated amplitude and phase contrasts increase with n, in itself an interesting result suggesting the usefulness of higher-harmonic demodulation. The calculated amplitude contrasts agree well with the measured ones, within 10%. The phase contrasts have a sign as predicted, but are about 3 times larger than calculated. This could arise from an incorrect choice of optical constants, but could also indicate a deficit of quasielectrostatic theory that may need to be extended to include retardation and radiation damping [16], or could indicate a redshift of the resonance in Fig. 2, expected when modifying Eq. (1) to describe an extended (Mie) rather than a point (Rayleigh) scatterer.

In summary, the studies reported here expand former observations [1,8,14] of optical superresolution from tip scattering. We demonstrate that the complex optical near-field response is obtainable on a nanometer scale, provided that interferometric detection is complemented by harmonic demodulation. The results show that the observed material contrast, both in amplitude and phase, can be explained by the complex optical constants using quasielectrostatic theory. This theory also describes the "surface enhanced" response induced by a metal tip [8], and perspectively applies to nonlinear interactions such as four-wave mixing that can benefit from the tip's field concentration [17]. Thus near-field microscopy may permit the investigation of optical susceptibilities at diminishing sample size, the detection of discrete electronic states, or quantum-size optical effects. Interesting objects are small metal and semiconductor particles well known to possess optical resonances which strongly depend on size and shape. Finally, we suggest raising the heterodyne s-SNOM's potential by using infrared wavelengths, since then increased metal conductivity improves the tip's antenna function, and since interference periods become even further separated from the near-field scale, and, last but not least, since important infrared material excitations, from atom vibrations [8] to electron gyrations [18], will become exploitable for nanoscience.

We thank B. Knoll, R. Guckenberger, and D. v. d. Weide (Madison) for stimulating discussions. This work was supported by BMBF.

*Electronic address: keilmann@biochem.mpg.de

[1] F. Zenhausern, Y. Martin, and H. K. Wickramasinghe, Science **269**, 1083 (1995).
[2] M. Fee, S. Chu, and T. W. Hänsch, Opt. Commun. **69**, 219 (1989).
[3] F. Keilmann, D. W. v. d. Weide, T. Eickelkamp, R. Merz, and D. Stöckle, Opt. Commun. **129**, 15 (1996).
[4] B. Knoll, F. Keilmann, A. Kramer, and R. Guckenberger, Appl. Phys. Lett. **70**, 2667 (1997).
[5] C. Gao, T. Wei, F. Duewer, Y. Lu, and X. D. Xiang, Appl. Phys. Lett. **71**, 1872 (1997).
[6] R. Carminati, Phys. Rev. E **55**, R4901 (1997).
[7] Such near-field phase images can be directly recorded by interferography, F. Keilmann, K. W. Kussmaul, and Z. Szentirmay, Appl. Phys. B **47**, 169 (1988).
[8] B. Knoll and F. Keilmann, Nature (London) **399**, 134 (1999).
[9] I. S. Averbukh, B. M. Chernobrod, O. A. Sedletsky, and Y. Prior, Opt. Commun. **174**, 33 (2000).
[10] B. Knoll and F. Keilmann, Opt. Commun. **182**, 321 (2000).
[11] E. A. Ash and G. Nicholls, Nature (London) **237**, 510 (1972).
[12] G. Wurtz, R. Bachelot, and P. Royer, Eur. Phys. J. Appl. Phys. **5**, 269 (1999).
[13] A. Lahrech, R. Bachelot, P. Gleyzes, and A. C. Boccara, Opt. Lett. **21**, 1315 (1996).
[14] H. F. Hamann, A. Gallagher, and D. J. Nesbitt, Appl. Phys. Lett. **73**, 1469 (1998).
[15] In this case the "z-motion" artifact cannot be completely avoided, since in the limit of large n or after subtracting background [14] one still measures a prime term $s_0^b s_n \cos(\varphi_0^b - \varphi_n)$ which is not the near field but merely a product of (a z-dependent) background with the near field.
[16] V. A. Markel, J. Mod. Opt. **39**, 853 (1992).
[17] J. Wessel, J. Opt. Soc. Am. B **2**, 1538 (1985).
[18] R. Merz, F. Keilmann, R. J. Haug, and K. Ploog, Phys. Rev. Lett. **70**, 651 (1993).